*Biochimica et Biophysica Acta*, 1059 (1991) 37–44

*ADONIS* 000527289100177G



BBABIO 43446

# Structural characterization of heme sites in spinach cytochrome $b_6f$ complexes: a resonance Raman study

J. David Hobbs [1], Max Wynn [2,*], David J. Nunez [1], Richard Malkin [2], David B. Knaff [3] and Mark R. Ondrias [1]

[1] *Department of Chemistry, University of New Mexico, Albuquerque, NM (U.S.A.),*
[2] *Division of Molecular Plant Biology, University of California at Berkeley, Berkeley, CA (U.S.A.)*
*and* [3] *Department of Chemistry & Biochemistry, Texas Tech University, Lubbock, TX (U.S.A.)*

(Received 27 November 1990)
(Revised manuscript received 25 March 1991)

Key words: Cytochrome $b_6f$; Resonance Raman; Photoreduction; Heme; Cytochrome $f$

**Resonance Raman spectra of cytochrome $b_6f$ complexes isolated from spinach chloroplasts have been obtained. Selective resonance enhancements and partial reductions of the complex by redox mediators were used to isolate and identify the contributions of heme $b_6$ and heme $f$ sites to the observed spectra. Corresponding spectra for turnip cytochrome $f$ have also been obtained. Power-dependent photoreduction was observed in cytochrome $f$ of the complex as well as in the isolated cytochrome $f$ during the course of the Raman experiments.**

## Introduction

The two photosystems operative in the oxygenic photosynthesis of chloroplasts are connected by a membrane-bound protein complex comprised of *b*- and *c*-type hemes and a high-potential [2Fe-2S] center. This so-called cytochrome $b_6f$ complex catalyzes the oxidation of plastoquinol by the copper protein plastocyanin and is also a site of proton pumping across the thylakoid membrane [1–3]. These complexes are structurally and functionally analogous to the cytochrome $bc_1$ complexes, which have been isolated from mitochondrial as well as photosynthetic bacterial sources.

Differences in the local heme environments (most notably heme axial ligation and direct protein/heme interactions) undoubtedly account for the wide variability in functionality among heme proteins. A wide array of physical techniques can be employed to probe heme active sites directly and indirectly. However, some intrinsically high information content techniques, such as X-ray crystallography and NMR, cannot generally be applied to large membrane-bound protein complexes. In contrast, resonance Raman spectroscopy (RRS) is easily applied to these multi-component systems, and the vibrational spectra produced by this technique contain an abundance of structural information.

The application of resonance Raman spectroscopy to multi-heme, electron transfer proteins is a relatively recent phenomenon. However, in view of the past successes of RRS in defining the structural and functional dynamics of single heme proteins such as cytochrome *c*, myoglobin and cytochrome *c* peroxidase [4–6] as well as multi-heme proteins such as hemoglobin and cytochrome *c* oxidase [7,8], the application of RRS to multiple, heteroheme proteins is a quite natural extension of the technique. Previously published Raman studies of membrane associated spinach oxidoreductases focused on the isolated cytochromes of the complex [9,10]. Our experiments seek to expand upon these studies by examining the individual components within the enzymatically active complex.

We have previously employed RRS in characterizing the heme sites of the cytochrome $bc_1$ complex isolated from the purple bacteria *Rhodosprillum rubrum* [11]. In this oxidoreductase, the three hemes present (cytochromes $c_1$, $b_h$ and $b_L$) differ in midpoint redox potentials so as to allow sequential titration of the hemes [12]. However, while the midpoint potentials of the two *b*-type hemes extant in the isolated complex differ slightly ($\Delta E_m \approx 50$ mV), their redox potentials are more homogeneous than those observed for cytochromes $b_h$

* Present address: Department of Biochemistry, University of Texas, Southwestern Medical Center at Dallas, Dallas, TX, U.S.A.

Correspondence: M.R. Ondrias, Department of Chemistry, University of New Mexico, Albuquerque, NM 87131, U.S.A.

and $b_L$ in photosynthetic bacteria [3]. Thus, in the $b_6f$ complex, redox titration is not as effective in separating the relative contribution of each heme type to the Raman spectrum. Therefore, in this study we were able to examine only three stages of heme reduction within the complex: fully reduced (cyt $f$(II) cyt $b$(II), fully oxidized (cyt $f$(III) cyt $b$(III)) and partially reduced (cyt $f$(II) cyt $b$(III)). Additionally, we have attempted to exploit differences in the heme absorptions for the two heme types of the fully reduced complex to selectively enhance the Raman spectrum of one heme type over the other.

## Materials and Methods

The spinach cytochrome $b_6f$ complex was purified by using the detergent octyl glucoside by the method of Black et al. [13] and Willms et al. [14] and stored in liquid nitrogen until needed. Turnip and spinach cytochrome $f$ and equine cytochrome $c$ (Type VI) were purchased from Sigma and used without further purification.

Samples were prepared for Raman spectroscopy by concentrating the purified cytochrome complexes in an Amicon Centricon 30 microconcentrator to a final concentration of about 100 $\mu$M in cytochrome $f$ and then transferred to an anaerobic optical cell to which reductants or oxidants could be added. Cytochrome $f$ was reduced by sodium ascorbate. The fully reduced complexes were obtained by addition of a few grains of dithionite. All reduced samples were degassed and kept under a positive $N_2$ atmosphere. Heme reduction was monitored by UV-visible absorption spectroscopy prior to, and following, each Raman experiment by using an HP8452 diode array spectrophotometer. All samples were cooled to about 10°C by a stream of refrigerated $N_2$ while exposed to laser light. Raman spectra were obtained by using a Molectron UV-24 nitrogen-pumped dye laser (tunable range from 380 to 830 nm) with an approx. 170 degree backscattering collection geometry. Average laser energy density was varied between 10 and 100 mJ/cm$^2$. Photoreduction of cytochrome $f$ was avoided by utilizing cylindrical focusing optics during data acquisition. The scattered light was focused into a SPEX 1403 double monochromator with an attached water-cooled photomultiplier tube (Hamamatsu R928). The spectral bandpass was 6–10 cm$^{-1}$ for all experiments. Raman shift frequencies were calibrated by comparison to a Raman spectrum of a benzene sample obtained just prior to data collection.

## Results

Raman excitations within the B-band (406–430 nm) of the heme absorption enhance polarized ($A_{1g}$) and depolarized ($B_{1g}$, $B_{2g}$) Raman active modes corresponding to in-plane metalloporphyrin ring vibrations [15]. In the high-frequency region (1100–1700 cm) of the Raman spectrum, the positions of these bands are reliable indexes for monitoring the oxidation, spin-state, and axial ligation of the heme iron [16,17].

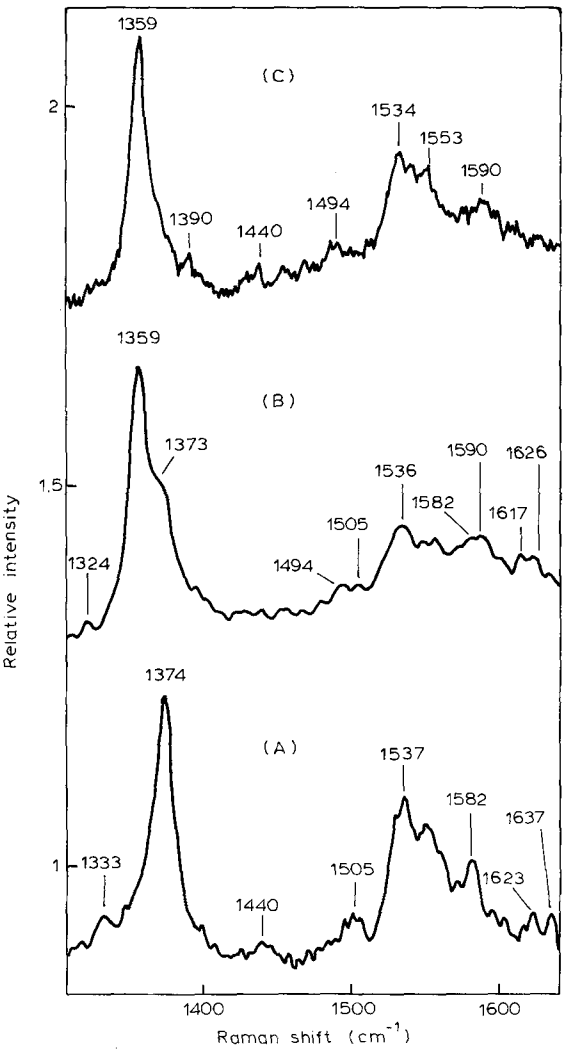


Fig. 1. High-frequency resonance Raman spectra of cytochrome $b_6f$ complexes isolated from spinach chloroplasts. (A) Potassium-ferricyanide-oxidized; (B) sodium-ascorbate-reduced; and (C) sodium-hydrosulfite-reduced. The excitation wavelength is 406 nm, with an average laser power of 3–4 mW at 15 Hz. Spectra are the average sum of 3–5 scans and have been smoothed by using a 21-point Savitsky-Golay smoothing routine. All samples are about 100 $\mu$M in cytochrome $f$ in 30 mM Tris-succinate (pH 6.5) and 30 mM octyl glucoside.

In Fig. 1, we present resonance Raman spectra obtained by using 406 nm excitation for the (A) ferricyanide oxidized, (B) ascorbate-reduced and (C) dithionite-reduced spinach cytochrome $b_6f$ complex. The corresponding absorption spectra are plotted in Fig. 3. Raman spectra in Fig. 1A and 1C are consistent with complete oxidation and reduction, respectively, of all heme sites of the complex. The symmetric pyrrole

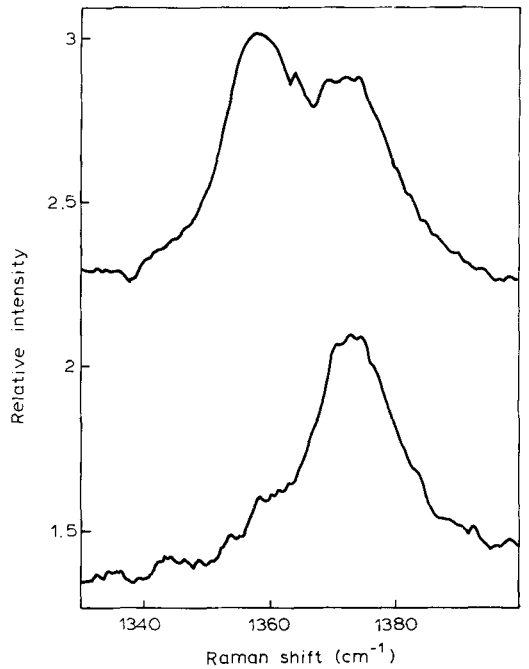


Fig. 2. These spectra demonstrate transient photoreduction in the ferricyanide-oxidized $b_6f$ complexes at 3 mW average laser power. The bottom spectrum was obtained by using cylindrical focusing optics. The top spectrum was obtained by using spherical focusing optics. All other sample and spectral conditions were the same as in Fig. 1.

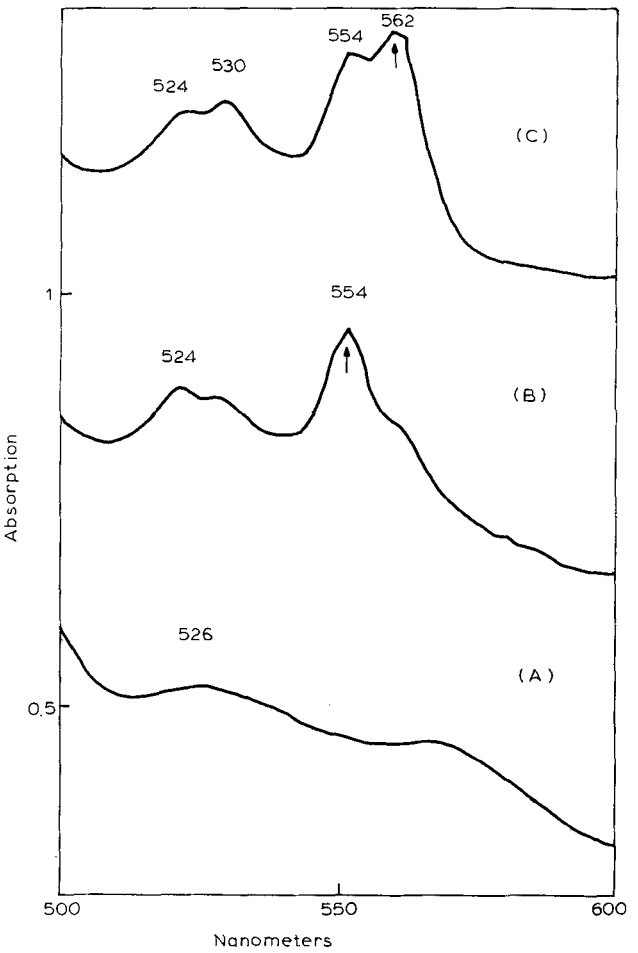


Fig. 3. UV-visible absorption spectra of the (A) potassium-ferricyanide-oxidized, (B) sodium-ascorbate-reduced and (C) sodium-dithionite-reduced spinach cytochrome $b_6f$ complexes. Vertical arrows denote two of the Raman excitation frequencies used in this study. All sample conditions were the same as in Fig. 1.

stretching mode, $\nu_4$, was observed at 1374 cm$^{-1}$ for the fully oxidized complex and at 1359 cm$^{-1}$ for the reduced complex. At moderate laser fluences (3 mW), heme photoreduction was observed in cytochrome *f* (see Fig. 2), as indicated from the presence of the

TABLE Ia

*Raman shift frequencies (in wavenumbers) for R. rubrum, cytochrome $bc_1$ and spinach cytochrome $b_6f$ complexes*

| | $bc_1$ | | $bc_1$ | | $bc_1$ | | $b_6f$ | | $b_6f$ | | $b_6f$ | |
|---|---|---|---|---|---|---|---|---|---|---|---|---|
| | $c_1$III | *b*III | $c_1$II | *b*III | $c_1$II | *b*II | *f*III | *b*III | *f*II | *b*II | fII | bIII |
| $\nu_4$ | 1373 | | 1362 | 1371 | 1360 | 1362 | 1374 | | 1359 | 1373 | 1359 | |
| $\nu_2$ | 1581 | | 1590 | 1583 | 1590 | 1582 | 1582 | | 1590 | 1582 | 1590 | |
| $\nu_3$ | 1505 | | 1494 | 1504 | 1491 | 1493 | 1505 | | 1505 | 1494 | 1490 | |
| $\nu_{10}$ | 1630 | 1624 | 1621 | 1621 | 1621 | 1617 | 1637 | 1623 | 1626 | 1617 | 1620 | |
| $\nu_{19}$ | – | | – | | 1589 | 1585 | – | | – | – | 1585 | 1586 |
| $\nu_{11}$ | – | | – | | 1542 | 1536 | – | | – | – | 1533 | 1533 |

TABLE Ib

*Some Raman shift frequencies (in wavenumbers) for cytochrome c, cytochrome $b_5$ and cytochrome f*

| | cyt*c*II | cyt*c*III | cyt$b_5$II | cyt$b_5$III | cyt*f*II | cyt*f*III |
|---|---|---|---|---|---|---|
| $\nu_4$ | 1362 | 1374 | 1362 | 1375 | 1357 | 1373 |
| $\nu_2$ | 1590 | 1586 | 1586 | 1581 | 1590 | 1588 |
| $\nu_3$ | 1493 | 1502 | 1494 | 1507 | 1490 | 1505 |
| $\nu_{10}$ | 1622 | 1636 | 1617 | 1619 | – | 1637 |
| $\nu_{19}$ | 1585 | 1582 | 1586 | 1587 | 1586 | – |
| $\nu_{11}$ | 1547 | 1563 | 1539 | – | 1538 | – |

approx. 1359 $cm^{-1}$ band in the spectra of samples that had been fully oxidized by treatment with ferricyanide prior to illumination. Absorption measurements indicated that sodium ascorbate reduces only the cytochrome *f* component of the spinach $b_6f$ complex. Thus, in Fig. 1B, $\nu_4$ was observed at 1359 $cm^{-1}$ with a shoulder at 1373 $cm^{-1}$. The positions are indicative of reduced cytochrome *f* and the oxidized *b*-type hemes, respectively. In addition, no photoreduction was observed in the ascorbate-reduced cytochrome $b_6f$ complexes in which cytochrome *f* is completely reduced. Thus, the band at 1359 $cm^{-1}$ in the preoxidized sample can be attributed to photoreduction of cytochrome *f*. The 1500–1600 $cm^{-1}$ region of the Raman spectra of the cytochrome complex is dominated by an intense mode centered at about 1537 $cm^{-1}$. This mode may be assigned to adventitious chlorophyll, based on its increased relative intensity when the Raman excitation is tuned in near resonance with the reported chlorophyll absorption maximum (440 nm) [18]. The presence of chlorophyll may have also been responsible for the large amount of background fluorescence observed when collecting the Raman spectra in this region. Other Raman bands assigned to the hemes of the complex are summarized in Table I.

The Raman spectra of turnip (Fig. 4) and spinach (data not shown) cytochrome *f* were obtained for comparison to spectra of the $b_6f$ complex obtained under similar conditions. Using B-band Raman excitation, we observe Raman modes $\nu_4$, $\nu_3$ and $\nu_2$ at 1373, 1505 and 1588 $cm^{-1}$ (Fig. 4A) for the oxidized cytochrome and at 1357, 1490 and 1590 $cm^{-1}$ (Fig. 4B), respectively, for the reduced species. Both turnip and spinach cytochrome *f* were found to be photoreducible (inset Fig. 4) at moderate laser powers even in the presence of ferricyanide.

Fig. 5 illustrates the effects of tuning the laser frequency to the $Q_0$ electronic absorption bands of the two heme types present within the $b_6f$ complexes. Resonance Raman spectra excited within the heme $\alpha$-band are dominated by non-totally symmetric and anti-symmetric, in-plane vibrations [19]. In Fig. 5B and C, we show the Raman spectra for the fully reduced cytochrome $b_6f$ complex enhanced at 550 and at 560 nm, respectively. These wavelengths correspond approximately to absorption maxima for reduced cytochrome *f* and $b_6$ (Fig. 3B and 3C). For comparison, Raman spectra of isolated turnip cytochrome *f* (Fig. 5A) and mitochondrial cytochrome $b_5$ (Fig. 5D) obtained under similar conditions, are also plotted. These results are summarized in Table I. In contrast to the behavior of *R. rubrum* cytochrome $bc_1$ complexes [11], no experimentally significant frequency shifts in the two most prominent modes, $\nu_{11}$ (1533 $cm^{-1}$) and $\nu_{19}$ (1586 $cm^{-1}$), are observed with a change in Raman excitation from 550 nm (Fig. 5B) to 560 nm (Fig. 5C).

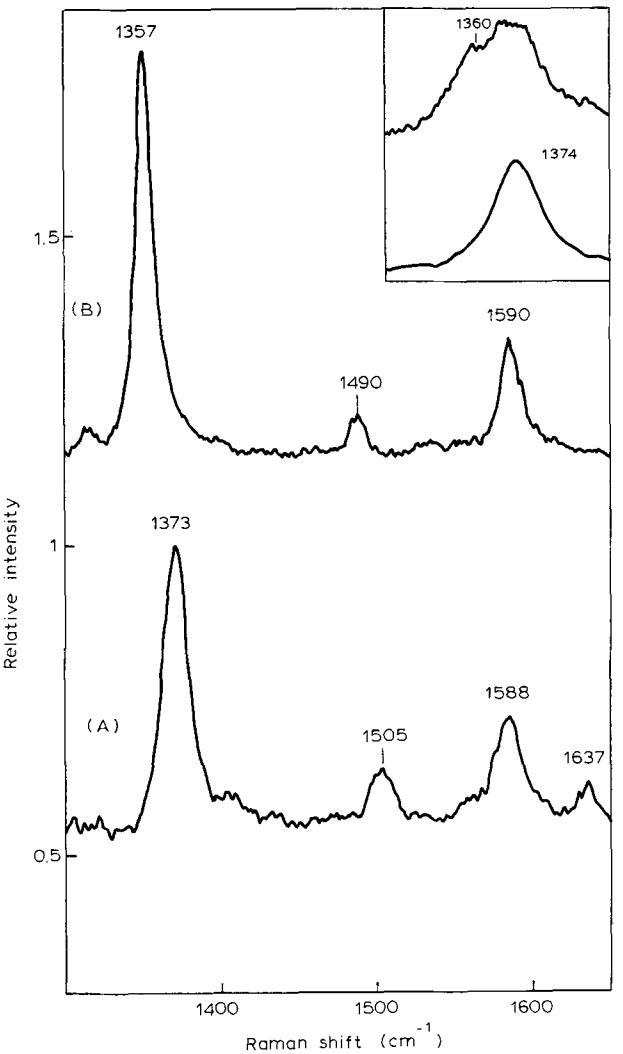


Fig. 4. High-frequency resonance Raman spectra of (A) ferricyanide-oxidized and (B) sodium-dithionite-reduced turnip cytochrome *f*. The inset spectra in the figure demonstrate photoreduction in the ferricyanide-oxidized cytochrome *f* under spectral conditions similar to those in Fig. 1.

In general, the quality of the spectra obtained for the cytochrome $b_6f$ complex is poorer than that of the spectra obtained previously for bacterial cytochrome $bc_1$ complexes, probably due to background chlorophyll fluorescence. In an attempt to reduce background fluorescence, cytochrome $b_6f$ complexes isolated by using two different preparatory procedures [13,14] were studied. However, no significant decrease in background fluorescence was observed and vibrational band positions and relative intensities were unchanged. Despite these higher backgrounds, some discernible changes in the spectra occur as the excitation wavelength is varied. In particular, the appearance of bands at about 1339 $cm^{-1}$ in Fig. 5C and D are diagnostic for heme *b* vinyl groups [20], while the bands at 1314 $cm^{-1}$ ($\nu_{21}$) and

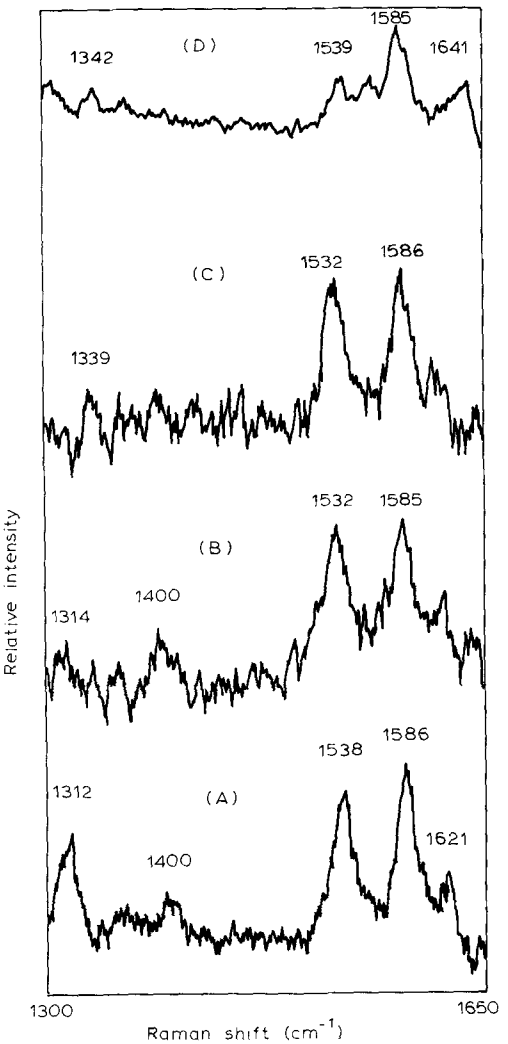


Fig. 5. High-frequency resonance Raman spectra of sodium-dithionite-reduced (A) turnip cytochrome *f* (550 nm excitation), (B) cytochrome $b_6f$ complexes (550 nm excitation), (C) cytochrome $b_6f$ complexes (560 nm excitation), and (D) mitochondrial cytochrome $b_5$ (550 nm excitation). Spectra are the averaged sum of four or five scans at an average laser power of 4 mW. All sample conditions were the same as in Fig. 1.

about 1400 $cm^{-1}$ ($\nu_{20}$) in Fig. 5A and D correspond with those observed for *c*-type cytochromes [21].

## Discussion

The subunit compositions of cytochrome $bc_1$ and $b_6f$ complexes isolated from bacterial and plant sources are much simpler than those found in mitochondria. In general, they consist of only 3–4 peptide subunits containing cytochromes *b*, $c_1$ and a Rieske [2Fe-2S] protein, respectively, while mitochondrial complexes contain 7–8 subunits [3]. Although the primary structures for a variety of these subunits are known [23], their tertiary and quaternary structures can only be inferred. These inferences, however, can be indispensable in sorting out the overall protein structure. For example, the cytochrome-*b*-containing peptides have all been shown to possess four conserved histidine residues in hydrophobic regions of the sequence. These histidines serve to provide bis-histidine ligation to the two *b* hemes of the complex [23]. Cytochrome *f*, like cytochrome *c*, exhibits a -Cys-X-X-Cys-His- sequence near the N-terminus that can bind the porphyrin via thioether linkages to the $R_2$- and $R_4$-positions of pyrrole group I and II, respectively, with the histidyl imidazole coordinating the heme iron. In contrast to cytochromes *c* and $c_1$, cytochrome *f* lacks a conserved methionine that could easily function as a sixth ligand in the heme binding region of the sequences. This finding has led to several proposals that a lysine residue is the sixth iron ligand [10,24,25,26]. In this study, we seek to employ RRS to compare the effects of axial ligation on the heme *b* and heme *c* vibrational properties in both intact $b_6f$ complexes and isolated cytochrome *f*.

*Fully reduced and oxidized complexes*

Raman spectra of the ferricyanide oxidized and dithionite reduced $b_6f$ complexes are consistent with complete oxidation and reduction, respectively, of the three hemes of the complex. The Raman mode most sensitive to heme iron oxidation state $\nu_4$ appears at 1375 $cm^{-1}$ (Fig. 1) for the oxidized and at 1359 $cm^{-1}$ for the reduced complex. Surprisingly, the full width at half maximum (FWHM) of $\nu_4$ for the fully reduced complex is 12 $cm^{-1}$. This value is similar to those reported for single heme proteins such as equine ferrocytochrome *c* at room temperature [27]. Thus, the $\nu_4$ bands for the ferric and ferrous cytochromes *f* and $b_6$ in the complex are coincident in position and have comparable linewidths. This is somewhat unexpected given the range of $\nu_4$ positions (1368 $cm^{-1}$ to 1376 $cm^{-1}$ for $Fe^{3+}$ and 1346 $cm^{-1}$ to 1364 $cm^{-1}$ for $Fe^{2+}$) among heme proteins exhibiting differences in porphyrin substituents, axial ligands and protein/heme bonding interactions (general Ref. 36).

Even in the presence of excess ferricyanide, a large fraction (more than 50% of the sites probed) of the cytochrome *f* hemes were photoreducible, as evidenced (Fig. 2) by an increase in the intensity of the approx. 1360 $cm^{-1}$ band at moderate to high laser fluences. Although we have previously reported photoreduction in a photosynthetic bacterial cytochrome $bc_1$ complex [11], the extent of photoreduction observed for the spinach $b_6f$ complexes is significantly greater. We speculate that this effect may be due to the presence of chlorophyll, which is in approx. 1 : 1 molar ratio with cytochrome *f* (based on a bacteriochlorophyll extinction coefficient of approx. 27.6 $mM^{-1}$ $cm^{-1}$ at 665 nm). In the bacterial complex previously investigated in our laboratory, the bacteriochlorophyll : cytochrome $c_1$ ratio was typically $< 0.2$ [12]. Other

factors (see below), however, may account for what is a fairly common phenomenon observed in heme proteins, especially membrane-solubilized oxidases [28,29].

The positions of Raman bands observed in the 1500–1700 $cm^{-1}$ region of the Raman spectrum have been demonstrated to be reliable indicators of the spin-state for either the ferrous or ferric heme iron [16]. For the oxidized $b_6f$ complex (Fig. 1), three such modes are readily discernible: $\nu_3$ (1502 $cm^{-1}$), $\nu_2$ (1582 $cm^{-1}$) and $\nu_{10}$ (1623/1637 $cm^{-1}$). The positions of these modes are approximately congruent with those found for ferricytochrome *c*: $\nu_3$ (1502 $cm^{-1}$), $\nu_2$ (1582 $cm^{-1}$) and $\nu_{10}$ (1636 $cm^{-1}$), as well as ferricytochrome $b_5$: $\nu_3$ (1507 $cm^{-1}$), $\nu_2$ (1581 $cm^{-1}$) and $\nu_{10}$ (1619 $cm^{-1}$). A similar pattern was observed in the Soret-enhanced spectrum of the fully reduced complex (see Table I). Thus, the presence of any high-spin cytochrome $b_6$ induced by denaturation and previously observed in EPR studies [30] may be ruled out.

Laser excitation within the heme $Q_{00}$ or $Q_{01}$ heme absorption bands produces Hertzberg-Teller scattering [19], which is predicated upon vibronic coupling of the B and Q electronic transitions. The Raman bands observed by using Q band excitations are of $B_{1g}$, $B_{2g}$ and $A_{2g}$ symmetries, in contrast to the totally symmetric $A_{1g}$ modes, which dominate Raman spectra obtained with B-band excitations. We have previously reported that, for the fully reduced cytochrome $bc_1$ complex, spectral isolation of the two heme types proved more effective when Q-band excitations were employed [11]. This effect may be due to electronic differences in the sixth axial ligand of the *b* and $c_1$ cytochromes that indirectly affect the relative occupation of the molecular orbitals of the porphyrin macrocycle. For the cytochrome $bc_1$ complex, the presumed ligand configurations are His-Fe-His for cytochrome *b* and His-Fe-Met for cytochrome $c_1$. In particular, the identity of the sixth axial ligand measurably alters observed positions for $\nu_{11}$ [9,10,20]. For example, in the *R. rubrum* $bc_1$ complex, $\nu_{11}$ was assigned at 1536 $cm^{-1}$ for the *b*-type cytochromes and at 1542 $cm^{-1}$ for cytochrome $c_1$. However, our results for the spinach cytochrome $b_6f$ complex indicate that $\nu_{11}$ (1532 $cm^{-1}$) for cytochromes $b_6$ and *f* are probably coincident and significantly lower in frequency. These results suggest that the sixth axial ligands of cytochromes $b_6$ and *f* do not differ significantly in their bonding interactions with *d* orbital of the heme iron. On the face of it, this possibility seems unlikely; however, it may be that the imidazole of cytochrome $b_6$ is sterically hindered from an optimal bonding geometry. Thus the Fe–N (imidazole) bond would be foreshortened and the porphyrin core size increased. A significant change in core-size, however, is not supported by the positions of $\nu_2$, $\nu_3$ and $\nu_{19}$ (Table I). It therefore seems probable that electronic effects arising from axial ligation, not changes in the macrocycle geometry, are the dominant factors in the behavior of $\nu_{11}$.

*Partially reduced complexes / cytochrome f*

The Raman spectra of the ascorbate-reduced complex are consistent with a separation of the vibrational modes for the *c*- and *b*-type hemes. For example, $\nu_3$ (1494/1505 $cm^{-1}$), $\nu_2$ (1582/1590 $cm^{-1}$) and $\nu_{10}$ (1617/1626 $cm^{-1}$) are split into two bands each (Fig. 1B). These new bands (1494, 1590 and 1626 $cm^{-1}$) are located at positions similar to those of ferrocytochrome *c* ($\nu_3$ (1493 $cm^{-1}$), $\nu_2$ (1590 $cm^{-1}$) and $\nu_{10}$ (1624 $cm^{-1}$)). The remaining bands can then be identified with ferricytochrome $b_6$ and they compare well with those observed for mammalian ferricytochrome $b_5$ ($\nu_3$ (1502 $cm^{-1}$), $\nu_2$ (1581 $cm^{-1}$) and $\nu_{10}$ (1519 $cm^{-1}$)).

The Soret-enhanced Raman spectra of the isolated turnip cytochrome *f* (Fig. 4) are generally consistent with those obtained for other low-spin-type cytochromes (see Table I). On the other hand, $\nu_4$ (1357 $cm^{-1}$) for reduced cytochrome *f* is approx. 5 $cm^{-1}$ lower than that reported for reduced equine cytochrome *c*. This lowering may reflect an increase in energy of the Fe $e_g$ ($d_\pi$) orbital, thus allowing for greater Fe ($d_\pi$) → porphyrin $e_g$ ($\pi^*$) back-donation of electron density. Consequently, the force constants for this mode and others would be lowered. This increase in energy of the Fe ($d_\pi$) molecular orbitals may be induced through greater non-bonding interactions by the sixth axial ligand coordinating the heme iron. A similar explanation has been evoked to account for changes in the Raman spectra observed in an alkaline transition (pH ≈ 9.3) of equine cytochrome *c* where the sixth axial ligand, Met-80, is believed to be replaced by a lysine, possibly Lys-72 or Lys-79 [21,31]. Preliminary results from this laboratory indicate that there are no parallel alkaline transitions (to pH ≈ 11.0) for turnip cytochrome *f*. Interestingly, $\nu_{11}$ (1538 $cm^{-1}$) for the isolated cytochrome *f* differs from that observed for the complex. Although this value is within a range observed for cytochromes thought to possess His-Fe-Lys axial ligands [21,22,32], it does intimate that isolation of cytochrome *f* peptide from the complex affects the heme environment.

*Photoreduction*

The isolated spinach and turnip cytochrome *f* were also found to be photoreducible (inset Fig. 4), although to less an extent than that observed in the $b_6f$ complex. From UV-visible absorption results (data not shown), we observed no chlorophyll associated with the isolated turnip cytochrome *f*. This fact may support involvement of the chlorophyll in the relatively more efficient photoinduced electron transfer observed in the spinach $b_6f$ complex. We have previously reported photoreduction in the cytochrome $bc_1$ complexes iso-

lated from *R. rubrum* [11], which also contain no spectroscopically significant amounts of chlorophyll. Thus, while the presence of chlorophyll may be a sufficient condition for the observed photoactivity, it is clearly not a necessary one. Other factors, such as ligand field and protein environment, must contribute to photoreducibility of the heme.

It does seem clear, however, that heme photoreactivity can be correlated with excited electronic states of the macrocycle; for example, photopumping in either the B- or the Q-band was more effective in generating the photoreduced species. It is also evident that photoreduction occurs on a relatively fast timescale: competitive with reoxidation by ferricyanide. The power dependence of heme photoreduction and preliminary data obtained using a two-pulse, pump-probe protocol indicate that, in the cytochrome $b_6f$ complex, the photoreduced species is generated within the pulse width of the laser (10 ns). However, at present signal-to-noise ratios, it is unclear whether the Raman spectrum of the transient species is different from that of the chemically reduced heme. These results suggest the existence of a nearby endogenous electron donor which can couple with the $\pi \rightarrow \pi^*$ transition of the heme.

Previous studies of heme photoreducibility have focused on proteins possessing high-spin iron geometries such as oxidases (heme $a_3$) [28,29], metmyoglobin [33,34] and hemoglobin [35]. In particular, the histidyl axial ligand to the heme has been implicated as a donor in the charge-transfer mechanism. For instance, methemoglobin was observed to be photoreducible only in the presence of inositol hexaphosphate, which stabilizes the 'T-state' form of the protein [35] in which the iron-imidazole bond is constrained by a bending or tilting. Thus, histidine position may contribute to, or influence, heme photoreducibility. Our results demonstrate that photoreduction occurs efficiently in six-coordinate *c*-type heme proteins isolated from the membranes of bacteria and chloroplast. It is also evident that cytochromes $c_1$ and $f$, possess unique axial ligands and/or ligand orientations in comparison to other cytochromes *c*. It is interesting to speculate that it is these conditions which are the source of the heme photoactivity.

## Conclusion

The data obtained in this study show that the Raman spectra for heme $b_6$ and heme $f$ of the spinach cytochromes $b_6f$ complex may be isolated through the use of redox mediators and selective resonance enhancement. Furthermore, useful comparisons can be made between the Raman spectra of the isolated mitochondrial cytochrome $b_5$ and turnip cytochrome $f$ and that obtained for the complex. In particular, we observe significant shifts in the Raman modes associated with the axial ligand environment for the isolated cytochrome $f$ as compared to those found for the intact $b_6f$ complex. However, our data for each species are consistent with the His-Fe-Lys axial ligation scheme previously proposed for cytochromes $f$ isolated from a variety of sources. In particular, the isolated cytochrome $f$ has a unique axial ligand field as compared to either the cytochrome $f$ of the complex or that of other *c*-type cytochromes.

Rapid heme photoreduction has also been observed in both the isolated cytochrome $f$ and is localized on the cytochrome $f$ heme of the complex. Photoreduction of the heme is power- and wavelength-dependent. However, it is unclear at this time whether the photogenerated transient differs spectrally from that of the chemically reduced species.

## Acknowledgements

The authors thank Dr. Kevin A. Gray for preparation of the cytochrome $b_6f$ complexes utilized in the early portions of this work. The financial support of the NSF (DMB-8716033 to D.B.K.), NIH (GM-20571 to R.M.), and the NIH (GM-33330 to M.R.O.) is gratefully acknowledged.

## References

1 Bendall, D.S. (1982) Biochim. Biophys. Acta 683, 119–152.
2 Hope, A.A., Birch, S. and Matthews, D.A. (1987) Aust. J. Plant Physiol. 14, 47–57.
3 Furbacher, P.N., Girin, M.E. and Cramer, W.A. (1989) Biochemistry, 28, 8990–8998.
4 Cartling, B. (1983) Biophys. J. 43, 191–205.
5 Spiro, T.G. (1983) in Iron Porphyrins (Lever, A.B.P. and Gray, H.B., eds.), Part II, pp. 91–159, Addison Wesley, Reading, MA.
6 Dasgupta, S., Anni, H., Yonetani, T. and Rousseau, D.L. (1989) J. Biol. Chem. 264, 654–662.
7 Rousseau, D.L. and Friedman, J.M. (1488) in Biological Applications of Raman Spectroscopy, Vol. III (Spiro, T.G., ed.) pp. 133–216, Wiley, New York.
8 Babcock, G.T. (1988) in Biological Application of Raman Spectroscopy, Vol. III (Spiro, T.P,., ed.), pp. 244–346, Wiley, New York.
9 Kitagawa, T., Kyoguku, Y., Iizuka, T., Ikeda-Sato, M. and Yamanaka, T. (1975) J. Biochem. 78, 719–728.
10 Davis, D.J., Frame, M.K. and Johnson, D.A. (1988) Biochim. Biophys. Acta 936, 61–66.
11 Hobbs, J.D., Kriauciunas, A., Guner, S., Knaff, D.B. and Ondrias, M.R. (1990) Biochim. Biophys. Acta 1018, 47–54.
12 Kriauciunas, A., Yu, L., Yu, C.-A., Wynn, R.M. and Knaff, D.B. (1989) Biochim. Biophys. Acta 976, 70–76.
13 Black, M.T., Widger, W.B. and Cramer, W.A. (1987) Arch. Biochem. Biophys. 252, pp. 655–661.
14 Willms, I., Malkin, R. and Chain, R.K. (1987) Arch. Biochem. Biophys. 25, 248–258.
15 Spiro, T.G. and Li, X.-Y. (1988) in Biological Applications of Raman Spectroscopy, Vol. III (Spiro, T.G., ed.), pp. 1–38, Wiley, New York.
16 Spiro, T.G. and Strekas, T.C. (1974) J. Am. Chem. Soc. 96, 338–345.

17 Spiro, T.G., Strong, J.D. and Stein, T.C. (1979) J. Am. Chem. Soc. 101, 2648.
18 Schick, G.A. and Bocian, D.F. (1987) Biochim. Biophys. Acta 895, 127–154.
19 Clark, R.J.H. and Stewart, B. (1979) Struct. Bonding 36.
20 Kitagawa, T., Iizuka, T., Saito, M.I. and Kyogoku, Y. (1975) Chem. Lett. 849–852.
21 Cartling, B. (1988) in Biological Applications of Raman Spectroscopy, Vol. III (Spiro, T.G., ed.) pp. 1–38, Wiley, New York.
22 Hobbs, J.D., Larsen, R.W., Meyer, T.E., Hazzard, J.H., Cusanovich, M.A. and Ondrias, M.R. (1990) Biochemistry, 29, 4166–4174.
23 Hauska, G., Nitschke, W. and Herrmann, R.G. (1988) J. Bioenerg. Biomembr., 20, 211–228.
24 Simpkin, D., Palmer, G., Devlin, F., McKenna, M.C., Jensen, G.M. and Stephens, P.J. (1989) Biochemistry 28, 8033–8039.
25 Rigby, S.E., Moore, G.R., Gray, J.C., Gadsby, P.M., George, S.J. and Thomson, A.J. (1988) Biochem. J. 256, 571–577.
26 Siedow, J.N., Vickery, L.E. and Palmer, G. (1980) Arch. Biochem. Biophys. 203, 101–107.
27 Adar, F. (1978) J. Chem. Phys. Vol. 82, 230–234.
28 Adar, F. and Yonetani, T. (1978) Biochim. Biophys. Acta 502, 80–86.
29 Ogura, T., Yoshikawa, S. and Kitagawa, T. (1985) Biochemistry 24, 7746–7752.
30 Nitschke, W. and Hauska, G. (1987) Biochim. Biophys. Acta 892, 314–319.
31 Smith, H.T. and Millett, F. (1980) Biochemistry 19, 1117–1120.
32 Kihara, H., Hon-Nani, K. and Kitagawa, T. (1978) Biochim. Biophys. Acta 532, 337–346.
33 Sage, T.J., Morikis, D. and Champion, P.M. (1989) J. Chem. Phys. 90, 3015–3032.
34 Morikis, M., Champion, P.M., Springer, B.A., Egegerg, K.D. and Sligar, S.G. (1990) J. Biol. Chem. 265, 12143–12145.
35 Kitagawa, T. and Nagai, K. (1979) Nature 281, 503–504.
36 Felton, R.H. and Yu, N.-T. (1983) The Porphyrins, Vol. III, pp. 347–393, Academic Press, New York.